Turkish Journal of Electrical Engineering & Computer Sciences

http://journals.tubitak.gov.tr/elektrik/

Research Article

Turk J Elec Eng & Comp Sci
(2016) 24: 3724 – 3740

doi:10.3906/elk-1410-3

# Electric arc furnace power quality improvement by applying a new digital and predicted-based TSC control

**Mehdi TORABIAN ESFAHANI**[1,2], **Behrooz VAHIDI**[2,*]
[1]Department of Electrical Engineering, Shahid Ashrafi Esfahani University, Isfahan, Iran
[2]Department of Electrical Engineering, Amirkabir University of Technology, Tehran, Iran

**Received:** 01.10.2014 • **Accepted/Published Online:** 05.06.2015 • **Final Version:** 20.06.2016

**Abstract:** Static VAR compensators (SVC) can improve some of the power quality (PQ) indices such as voltage flicker, unbalances, and power factors in power systems if properly controlled. Different nonlinear and time-varying loads generate these parameters. One of the great nonlinear loads is the electric arc furnace (EAF), which causes waveform distortions, voltage unbalances, and fluctuations. In this paper, a new digital and prediction-based control for thyristor switched capacitors (TSCs) was proposed to compensate an actual steel industrial plant. The digital control was based on generating adequate synchronous pulses, calculating required suitable susceptance, and measuring correct reactive power. The proposed TSC improved the PQ by means of the feedback from voltage and power factor. A predictive method based on time series and recursive least square with dynamic learning factor was then applied to estimate EAF reactive power in the future so that the TSC performance was enhanced by reducing the natural time delay. A band-pass harmonic filter was designed to compensate the load current harmonics and to protect the capacitor banks in the TSC. Finally, the suggested TSC was implemented in a steel industrial plant as an actual power system with 2 EAFs. The modeling and experimental results indicate the effectiveness of the proposed TSC.

**Key words:** Electric arc furnace, power quality phenomena, thyristor switched capacitor compensator, harmonic filter, predictive method

## 1. Introduction

Operation of electric arc furnaces (EAFs) presents 2 important aspects making their study in power systems inevitable:

1. These loads are the largest electric loads that can actually affect other loads and other customers in power networks.
2. These loads can generate almost all the power quality parameters such as voltage unbalances, voltage fluctuations (in particular flicker), voltage, current harmonics, and interharmonics.

Therefore, it is essential to suggest a suitable model for EAFs that can create the expected effects in a power system. So far, numerous models of EAF have been presented by different researchers [1–5].

The voltage-source models based on voltage-current (V-I) characteristics were presented in [1], where voltage is usually considered as current equations related to V-I characteristics. In this model, a relation is required to modulate voltage for flicker generation. Also, a 2-step optimization technique was analyzed in [2] to

*Correspondence: vahidi@aut.ac.ir

identify the arc furnace parameters considering the stochastic nature of the arc length. This method is based on a genetic algorithm (GA) that adopts the arc current and voltage waveforms to estimate the parameters of the nonlinear time-varying model of an EAF.

The data-based models are based on data collection in actual power systems, which are not considered as black boxes for any EAF and are usually applied to studying PQ [3]. A frequency model was described for harmonic analysis in [4].

On the other hand, there are static compensators such as thyristor switched capacitors (TSCs), thyristor controlled reactors (TCR) known as static VAR compensators (SVCs), and a new descendant called the static synchronous compensator (STATCOM), which are usually employed to improve PQ parameters or reduce their destructive effects. Due to economic problems, customary SVCs are applied to compensate different PQ parameters such as reactive power and power factor [5–9].

An analysis of static compensators and a discussion of dynamics concerning this issue was provided in [5,6], where a comparison was summarily made among static compensators in terms of dynamic behavior, while nothing was mentioned about their control. Also, in [7,8], a specific example of a power system with an arc furnace was considered along with static compensators. The structure and performance of the TCR and STATCOM in reducing the voltage flicker of the EAF were also compared in [9]. A summarized discussion of measuring reactive power in a 3-phase power system was also briefly presented in [10,11]. The disadvantage of the mentioned system is that the stochastic error in the system is reinforced instantaneously, causing reduction of the speed and accuracy. Moreover, some explanations were provided in [12,13] regarding how to design harmonic filters in power systems with EAFs.

According to the above description, this paper followed the goals below:

1) A 3-phase power system with 2 EAFs established in the Khozestan Steel Company (KHSC) as an actual case study was modeled and compared with experimental results measured by PQ analyzer. The EAF model was based on the hidden Markov model (HMM) proposed in [5]. Therefore, the designed power system had a minimum error for the KHSC.

2) In the KHSC, a TSC was selected to compensate the reactive power. This compensator was composed of 2 separate capacitor banks to reduce the number of capacitor switchings. Therefore, it was necessary to optimize this compensator so that it could be used for all TSC abilities and for mitigated voltage fluctuations in the main bus of the power system. Hence, in this paper a new digital control for TSC was presented to measure quick changes of electric power with the correctness and accuracy desired. This control strategy consists of measuring reactive power and calculating the required capacitor susceptance instantaneously, as well as generating suitable synchronous pulses for thyristors without generating voltage and current transients.

3) For harmonic protection of the TSC, band-pass harmonic filters, installed parallel to the compensator, were used to reduce the effect of current harmonic distortion. Thus, the filters both reduced the effects of resonance in fundamental frequency and compensated the reactive power in this frequency.

4) The SVCs had a time delay between 1/2 or 1 cycle in natural operation, causing speed reduction of performance and nondesirable compensation. Hence, a new method based on autoregressive moving average (ARMA) and recursive least square with dynamic learning factor (RLS-DLF) was proposed in this paper for a reactive power estimates for the future.

5) A comparison was done between modeling and experimental results for validation analysis of the proposed method.

## 2. The design of a power system with 2 alternating current EAFs

The single-line diagram of the KHSC power system is represented in Figure 1. This company has 2 EAFs and 1 compensator per bus. The TSC improves the effects of the EAFs' operation. Table 1 shows the actual values of the KHSC power system.

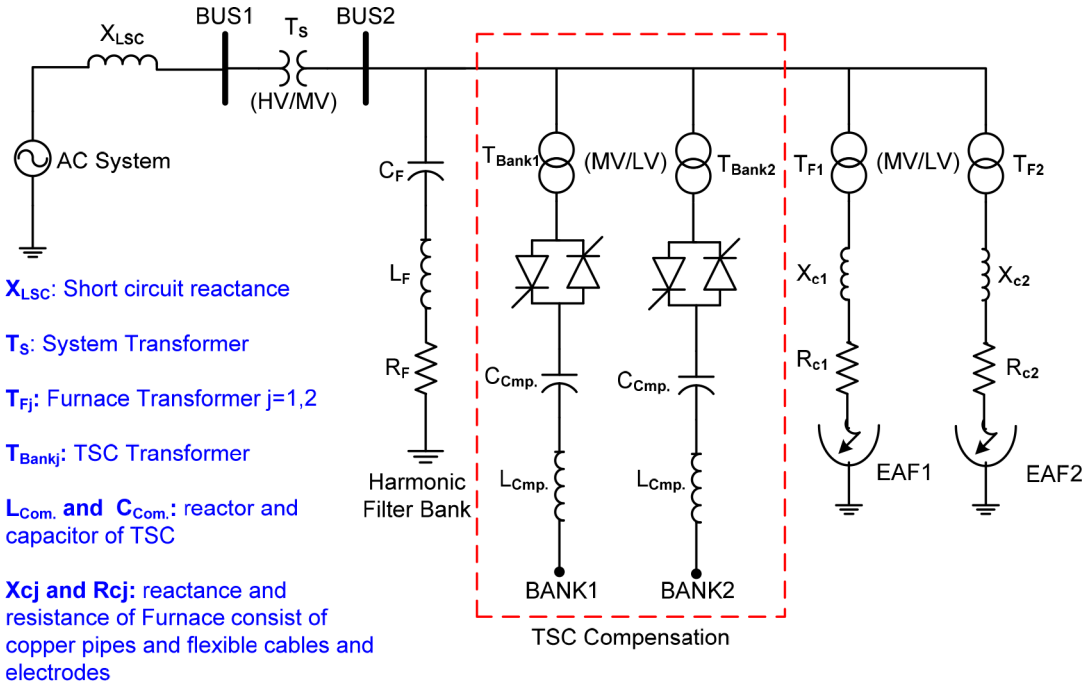


**Figure 1.** The schematic of the EAF supply system, together with the TSC compensator and harmonic filter.

**Table 1.** Different parameters of system and loads.

| Different parameters | |
|---|---|
| Supplying system | $S_{sc} = 11000MVA, V = 230kV, X_{th} = 14.5m\Omega, f = 50Hz$ |
| Arc furnace loads | Final values with flexible cables of electrodes and the electrode arms<br>$L_{c_1} = 4.0959\mu H + 3.32\mu H + 2.37\mu H = 9.7859\mu H$<br>$X_{c_1} = j3.074m\Omega$<br>$R_{c_1} = 71 + 129.7 + 3.55 = 204.25\mu\Omega$<br>$L_{c_2} = 4.168\mu H + 3.42\mu H + 2.43\mu H = 10.018\mu H$<br>$X_{c_2} = j3.092m\Omega$<br>$R_{c_2} = 73 + 123.7 + 4.05 = 200.75\mu\Omega$ |

In Figure 1, the TSC transformers reduce the voltage level on the capacitors and thyristors, $T_{Bank1}$ and $T_{Bank2}$ (MV/LV). As can be seen in this figure, to limit transients caused by switching, to decrease inrush currents, and to prevent resonance from within the power network, a small reactor in series with the capacitor is used. In the proposed design procedure, 2 separate capacitor banks were used to improve compensator

performance and to reduce switching. Each capacitor bank in this figure has $n$ varying capacitor steps based on load reactive power and 1 fixed capacitor step for steady state and adjusting the overall average power factor in each phase. Also, in the 3-phase circuit of the power system, the capacitor steps are connected in a triangle coupling manner to eliminate third-order harmonics.

### 2.1. The statistical-probabilistic model of an electric arc

As mentioned, arc modeling is important for power system analysis. Up to now, different models for EAFs have been suggested [1–4]. In this paper, with regard to the disadvantages of those models, the arc model was based on the statistical-probabilistic method employing the hidden Markov model (HMM) [5]. This model is based on system identification by considering a specific EAF so that the arc model is determined through sampling the arc current in the initial melting (scrap), mild melting, and refinement stages. After sampling the arc current in each stage of the furnace operation via oscilloscopes, the electric arc is modeled in the form of a voltage source dependent on the current by applying the HMM method. In other words, at any period of time in the experimental process, the arc voltage is obtained with respect to the value of arc current using the HMM. As a result, the V-I characteristic of the arc is completed. The advantage of this model in comparison to other models is its capability of describing the EAF behavior in the time domain in accordance with the actual arc with minimum error. To implement the HMM method, 2 Hioki-3196 measurement devices were connected to the PCC bus and bus 2 in order to record the active and reactive power as well as the harmonics of EAFs. Also, 2 oscilloscope devices were jointed to EAF1 and EAF2 to collect the voltage and current signals with a sampling period of 128 $mu$ s. In each step, measurements were compared with modeling to achieve the minimum error. It should be noted that all the measuring devices were synchronized together.

### 2.2. TSC compensator

Each step of the TSC included a capacitor, a bidirectional thyristor, and a small reactor. As mentioned above, this reactor was used initially to limit the surge current in the thyristor under irregular operations such as the capacitor switching at the wrong time due to control malfunction. It was also used to avoid resonances with the power system impedance at particular frequencies. Under the steady-state conditions, when the thyristor is closed and TSC branch is connected to the power supply, the current phasor in the branch is obtained as:

$$I = \frac{V_m}{X_{CCom.}} \cdot \frac{m^2}{m^2 - 1}, m = \sqrt{\frac{X_{C_{Comp.}}}{X_{L_{Comp.}}}} \tag{1}$$

The voltage amplitude across the capacitor is obtained as:

$$V_{CComp.} = \frac{m^2}{m^2 - 1} V_m \tag{2}$$

To generate the transient-free switching of the capacitors, Figure 2 is proposed. As can be seen, 2 simple laws govern all the possible conditions. The first law: if the residual capacitor voltage is lower than the system voltage peak ($V_{Capacitor} < V_m$), then the suitable instant for switching is when the voltage system is equal to the capacitor voltage. The second law: if the residual capacitor voltage is equal to or higher than the system voltage peak ($V_{Capacitor} \geq V_m$), then the correct switching is at the peak of system voltage, while thyristor voltage is minimum. Therefore, the maximum possible time delay in switching of a capacitor bank is 1 full-cycle of the system voltage (20 ms), which is the interval between the positive (negative) peak and the next positive

(negative) peak. It follows that the firing delay angle control is not suitable for the capacitors; the capacitor switching must take place at the particular instant when the voltage across the thyristor is zero or minimum. Accordingly, a TSC branch can provide only a step-like change in the reactive power (maximum or zero). To solve the above problem, in this paper it was proposed that $n$capacitor units in each bank be applied. Hence, the reactive power has a continuous waveform.

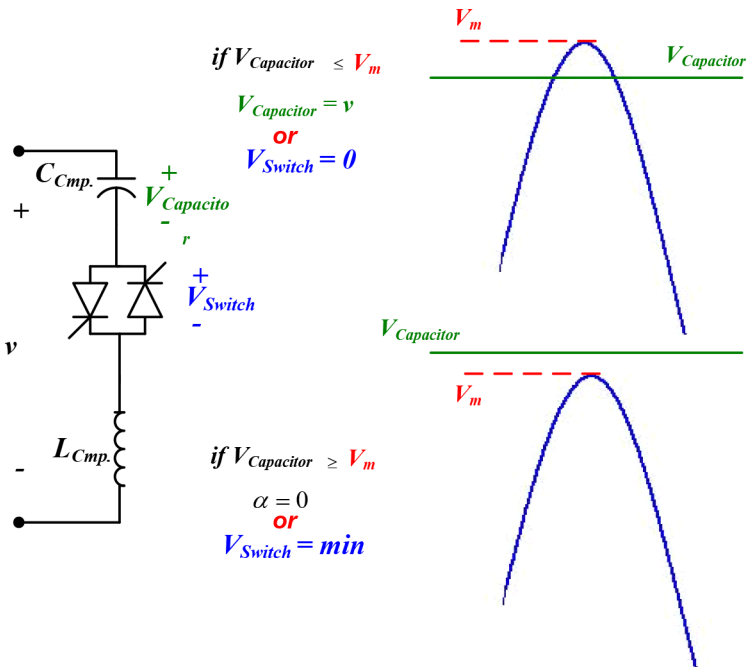


**Figure 2.** Transient-free laws for capacitor switching.

### 2.3. The harmonic filters design

The capacitor banks are very sensitive to harmonic currents. Even if the harmonic currents are very small, the resonance between the system impedance and the capacitor bank can amplify the harmonic currents. If the harmonic current frequency is the same as that of the power, a current amplification of the capacitor bank takes place, which may lead to its destruction. The best method for protection against such a breakdown is a shunt passive filter (including series capacitor and reactor). A shunt passive filter eliminates the harmonic currents from the supply system [14,15]. Moreover, in the power frequency, the shunt filter operates as a reactive power compensator. In this paper, a set of 2nd, 3rd, 4th, and 5th order harmonic filters were considered for the power system. The relations for these type of filters can be written as:

$$\begin{aligned} X_{L_F} &= L_F \cdot \omega_\circ \\ X_{C_F} &= \tfrac{1}{C_F \cdot \omega_\circ} \\ (m \cdot \omega_\circ)^2 &= \tfrac{1}{L_F \cdot C_F} \end{aligned} \tag{3}$$

The filter performance quality ($Q_F$) is computable from the following equation:

$$Q_F = \frac{m \cdot X_{L_F}}{R_F} \tag{4}$$

The reactive power of the filter in fundamental frequency is calculated as:

$$Q_{Fund} = Q_{C_F} - Q_{L_F} = \frac{|V_F|^2 \cdot (m^2 - 1)}{X_L \cdot \left[\left(\frac{n}{Q_F}\right)^2 + (1 - m^2)^2\right]} \tag{5}$$

where $\omega_0$ is the angular velocity in the fundamental frequency, $m$ is the harmonic order, and $R_F$, $L_F$, $C_F$ are the resistance, reactor, and the capacitance of the filter as shown in Figure 1, respectively. $V_F$ and $I_F$ are the filter voltage and current.

## 3. The proposed control TSC

The most important part of static compensators is their control system, which must have the necessary speed and accuracy to desirably perform the compensation. To achieve this goal, the control system is designed in 4 separate parts including reactive power measurement, generation of the required signal for the control system, computation of the required susceptance for compensation, and circuits designed for thyristor firing pulse generation. The different parts of the control system are shown in Figure 3. As shown in this figure, digital circuits are used in the control system to increase the performance speed. In the following, all parts are described in detail.

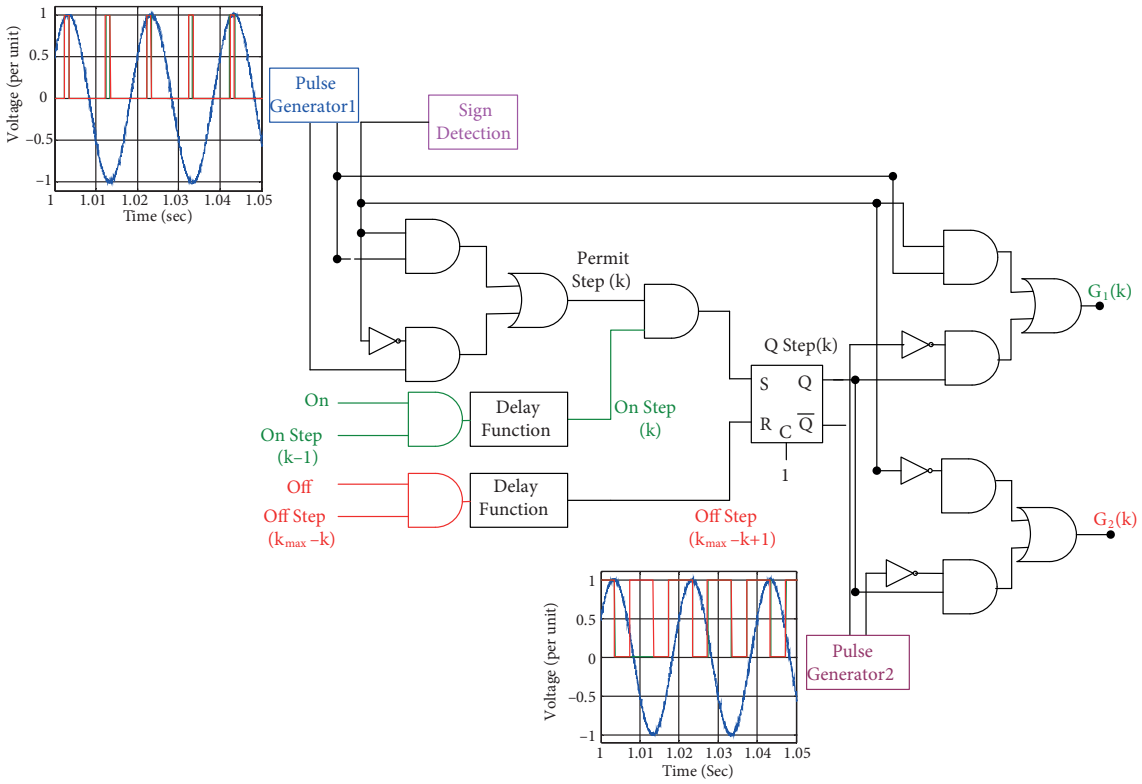


**Figure 3.** Proposed TSC control strategy.

With regard to Figure 3, 'step' denotes the capacitor units from 1 to k, 'sign detection' determines the sign of the capacitor voltage units, and 'delay function' prevents the different units from having any interference with each other.

### 3.1. The reactive power measurement unit

In general, the SVC uses the reactive power signal that precisely measures the fundamental reactive power of the EAF. This reactive power can be calculated per phase at one period so that in a continuous manner it is as follows [12,13]:

$$Q = \frac{1}{T}\int_{T} v(t'-\frac{T}{4})i(t')dt' \tag{6}$$

where $Q$ is measured by the reactive power in one period as indicated by $T$ and $v$ and $i$ are the voltage and the current in time domain $t'$, respectively. If voltage and current are measured in a discrete time, the reactive power can be obtained per phase at one period as follows:

$$\begin{aligned} &q_1(t) = \tfrac{1}{2T_d}\sum_{s=T_d(t-1)+1}^{T_d(t+1)} v(s-\tfrac{T_d}{2})i(s) \\ &t = 1,2,...,n, s = 1,2,...,m \end{aligned} \tag{7}$$

where $T_d$ denotes the number of samples per half-cycle, and $s$ is the sample number and $t$ marks time series components.

Eq. (6) provides a continuous signal for indicating the reactive power at one period, which has just completed at time $t$. In traditional static compensators, where there is no reactive power prediction, the fundamental reactive power that should be an up-to-date value is used for admissible compensation. In practice, it is accepted that an integration of one period interval is too high for flicker mitigation. Hence, the compensators usually apply a shorter integration interval such as a half-period integration. It should be noted that the reactive power calculation by any interval of integration besides the one period interval of integration cannot describe the fundamental reactive power because it is pulled down by current harmonic components $i$. Therefore, it can be said that using a half-period interval of integration leads to a corrupted accuracy causing the speed to flicker. Hence, to achieve optimal parameters for reactive power prediction, Eq. (7) and reactive power measurements in one period, similar to this equation, are applied for determining the best signal. Thus, not only is the fundamental reactive power adequately obtained but also the SVC speed performance is increased and the flicker can be reduced as well. Now, for estimating the reactive power in future, ARMA is proposed. In [16], the predicted reactive power based on different types of ARMA in second windows is suggested. Although this method has good results for predicting the reactive power, in practice this method cannot be applied for improving SVCs, because the SVC control system operates in a half period and the reactive power should be predicted at the same time by fast sampling data. Hence, in this section, an adequate time series based on ARMA is obtained. The ARMA (p,l) with all coefficients for reactive power is represented as follows:

$$\begin{aligned} q(t+1) \quad = \quad & r_{1,j-1}q_j(t) + r_{2,j-1}q_j(t-1) + \ldots + r_{p,j-1}q_j(t-p+1) \\ & -o_{1,j-1}a(t) + o_{2,j-1}a(t-1) + ... + o_{l,j-1}a(t-q+1) \end{aligned} \tag{8}$$

where $r$ and $o$ represent the model coefficients that have been predicted by the data of window *j-1*. The model is used to estimate $q(t)$ in window $j$. Windows $j$ and *j-1* depict the current and previous data windows, respectively, and $q(t)$ is the value of time series at time $t$ and $a(t)$ is a white Gaussian noise that is employed as an error between $q(t)$ and $q(t+1)$. The model coefficients $r_p$ are computed for the data windows with the length of a 1/2 cycle to 10 cycles. The time series of the model coefficients has white noise properties such that the coefficients' variations do not follow any specific law. Hence, updating the model coefficients is necessary

for prediction purposes by fast sampling methods and these coefficients can be updated by appropriate online methods. Therefore, RLS-DLF is proposed. This algorithm can update the coefficients very fast and follows the reactive power as well. It can be used for improving the TSC control system.

According to Eq. (7) and the sampling period, the different parameters are:

$$T_d = \ 78\ n = \ 1000\ m = 78125 \tag{9}$$

On the other hand, the results of data collection and the modeling system are simultaneously compared to achieve a precise model of power system that considers all of the states. First, this power system model has all of the EAFs' properties, and second, it has the desired accuracy in comparison with the actual data measured.

The coefficients of the behavior of ARMA models used for the EAFs' reactive power time series were investigated and it was demonstrated that updating the model coefficients was necessary for prediction purposes. For this purpose, we first considered Table 2, which shows the means and standard deviations of various coefficients of the ARMA models calculated for 1350 reactive power time series. The length of these time series is 10 s with small length windows of 1 cycle (20 ms). The great values of the standard deviations show that the model coefficients are different for various data records. It should be noted that for calculating the coefficients in different ARMA models, it is necessary to analyze the autocorrelation function (ACF) and partial autocorrelation function (PACF) of time series at each step to check the adequate ARMA. The related equations are given in Appendix A.

**Table 2.** Means and standard deviations of various models coefficients obtained for 1350 time series.

| ARMA Different models | | ARMA(2,1) | ARMA(3,1) | ARMA(2,2) | ARMA(3,2) |
|---|---|---|---|---|---|
| $r_1$ | Mean | 0.62 | 1.12 | 1.92 | 1.92 |
| | STD | 0.38 | 0.48 | 0.33 | 0.71 |
| $r_2$ | Mean | –0.18 | –0.42 | –0.92 | –0.82 |
| | STD | 0.15 | 0.11 | 0.41 | 0.65 |
| $r_3$ | Mean | | –0.12 | | 0.12 |
| | STD | | 0.17 | | 0.21 |
| $o_1$ | Mean | –0.36 | –1.12 | –0.92 | –0.52 |
| | STD | 0.12 | 0.2 | 0.51 | 0.82 |
| $o_2$ | Mean | | | 0.72 | 0.54 |
| | STD | | | 0.45 | 0.76 |

By considering Table 2, the ARMA (2,1) is selected for modeling the reactive power time series, and the prediction relationship is:

$$\hat{q}(t+1) = r_1 q(t) + r_2 q(t-1) + r_3 e(t) + r_4 \tag{10}$$

$$e(t) = q(t) - \hat{q}(t) \tag{11}$$

The average of the time series is denoted by $r_4$. Since the value of $r_4$ is much greater than the $r_1$, $r_2$, and $r_3$ values, it is set to $r_4' v$ with $v = 10^7$. Thus, in updating the process, $r_1$, $r_2$, $r_3$, and $r_4'$ are determined. The RLS-DLF algorithm previously designed is then applied to update the ARMA (2,1) coefficients.

Now, with regard to the above equation, the reactive power is predicted in the next t by an adaptive filter, RLS type. First the filter coefficients are determined based on the minimum mean square error (MMSE)

criterion method. In the MMSE criterion, linear combiners are used. The input vector and vector of weighting factors in the linear combiner are defined as follows:

$$X_k = \begin{bmatrix} x_1 & x_2 & ... & x_k \end{bmatrix}^T \tag{12}$$

$$\omega_k = \begin{bmatrix} \omega_1 & \omega_2 & ... & \omega_n \end{bmatrix}^T \tag{13}$$

where $k$ is the number of the input signals and $n$ is the number of the weighting factors. The error signal can be expressed as:

$$e_k = d_k - X_k^T \omega_k \tag{14}$$

where $d_k$ is the desired response of the system. Now the behavior performance function and error function can be respectively defined as follows:

$$\zeta_k = \sum_{i=1}^{k} \left[ d_i - \omega_k^T Z_i \right]^2 \tag{15}$$

$$\varepsilon_k = \sum_{i=1}^{k} \mu^{k-1} e_i^2 \tag{16}$$

where $\mu$ is the learning factor, which is between 0 and 1. In order to obtain the optimal weighting factors, it is sufficient to derive the behavior performance function in relation to the weighting factors vector and set it equal to zero. Hence, the autocorrelation function (AF) of input and cross-correlation function (CF) between the input and the desired signal should be obtained as:

$$AF_k = \sum_{i=1}^{k} \mu^{k-i} X_i X_i^T \tag{17}$$

$$CF_k = \sum_{i=1}^{k} \mu^{k-i} X_i d_i \tag{18}$$

The above equations can be written as follows:

$$AF_k = \mu R_{k-1} + x_k x_k^T \tag{19}$$

$$CF_k = \mu CF_{k-1} + x_k d_k \tag{20}$$

Therefore, the weighting factors at the optimal point can be calculated as:

$$\omega_k^T = \frac{CF_k}{AF_k} \tag{21}$$

The RLS method is based on a recursive algorithm and with regard to Eqs. (20) and (21), the input autocorrelation matrix can be written as follows:

$$AF_k^{-1} = \mu^{-1} AF_{k-1}^{-1} - \frac{\mu^{-2} AF_{k-1}^{-1} X_k X_k^T AF_{k-1}^{-1}}{1 + \mu^{-1} X_k^T AF_{k-1}^{-1} X_k} \tag{22}$$

By defining the following adaptation gain, the above equation can be rewritten as:

$$\phi_k = \frac{\mu^{-1} AF_{k-1}^{-1} X_k}{1 + \mu^{-1} X_k^T AF_{k-1}^{-1} X_k} \tag{23}$$

$$AF_{k-1}^{-1} = \mu^{-1} AF_{k-1}^{-1} - \mu^{-1} \phi_k X_k^T AF_{k-1}^{-1} \tag{24}$$

Therefore, the weighting factors in this method are:

$$\omega_k^T = CF_{k-1} AF_k^{-1} + X_k^T d_k AF_k^{-1} \tag{25}$$

Substituting Eq. (24) with (25), the weighting factors are:

$$\omega_k^T = \omega_{k-1}^T - \omega_{k-1}^T \phi_k X_k^T + X_k^T d_k AF_k^{-1} \tag{26}$$

According to the error signal in Eq. (14), the vector of the weighting factors is calculated as follows:

$$\omega_{k+1} = \omega_k + \phi_k e_k = \omega_k + AC_F^{-1} X_k e_k \tag{27}$$

The proof of Eq. (27) is given in Appendix B.

Although this parameter is small, old prediction errors will be quickly forgotten, i.e. if not utilized in determining the estimation. In general, $\mu$ is considered close to 1. In this paper, with regard to the intense changes in updating reactive power coefficients, at first $\mu$ is equal to 0.98. Then this parameter is dynamically obtained as in the following equation:

$$\mu_k = \mu_{k-1} - \lambda \nabla_\mu(k) \tag{28}$$

where $\lambda$ is the step size and $\nabla_\mu(k) = \nabla\mu(E\{e^2(k)\})$.

### 3.2. Generation of the required pulses

The capacitors' switching excites transient modes, which may be large or small, depending on the capacitor's resonance frequency. To minimize the voltage and current transients on the thyristors, it is necessary that the capacitors still stay in their maximum charge value after exiting from the circuit. To achieve this goal, synchronizing pulses of +1 and –1 ms width are generated according to the network voltage. These pulses begin from the instant before positive and negative network voltage peaks and continue to the voltage peak instant. The +1 ms pulses are generated for making charge-keeper pulses of capacitors with positive polarity; similarly, –1 ms pulses are created for making charge-keeper pulses of negative polarity capacitors. On the other hand, in this section, in order to generate the continuous fire pulses of thyristors, synchronizing pulses of +6 and –6 ms are produced according to the network voltage. These pulses are produced similar to 1 ms synchronizing pulses.

### 3.3. Calculation of the susceptance required

The control system should calculate the number of capacitor steps connected in each section and consequently the reactive power injected in the power system is computed. This reactive power includes the reactive power of passive filters, TSC branches, and EAFs. The sum signal of the load and the capacitance reactive power enters the comparing units (see Figure 3). If the sum signal is more than the positive amount of single-phase

capacitive reactive power, the 'connect' command is activated, resulting in the capacitive steps needed at each section entering the power system. If the sum signal is less than the negative amount of the single-phase capacitive reactive power, the 'cut' command is activated; therefore, the necessary number of capacitor steps exit from the circuit. Now, if the sum signal amount is between the 2 values mentioned above, then the control system issues no command. Also, to simultaneously prevent the entrance of all the steps to the circuits after activating the connect command, a time delay of about 50 $mu$ s is considered in the control system. Of course, this time delay is very small and has no effect on the compensator control speed.

After this stage, firing pulses are applied to each thyristor while considering the command signal and 6 ms synchronic pulses. When the controlling command is deactivated, the pulses fired to the thyristors are stopped. The proposed control prevents the compensating system from producing harmonics in the system in addition to the mentioned advantages.

## 4. Experimental results

By considering Figure 1 and Table 1, the voltage-current characteristic curve of the furnace is illustrated in Figure 4a. The 3-phase voltage changes in the secondary furnace transformer in one complete melting cycle are shown in Figure 4b. A comparison is made between the modeled KHSC power system and the actual data collected by PQ measurement in Figure 4c. As seen in this figure, the error between the modeling and the measurement results is very low.

The effects of reactive power compensation on power quality phenomena in the power network with regard to the usual and proposed TSC, as shown in Figure 1, were analyzed and studied. Before performing the evaluation, different parameters of the predictive method were investigated. Hence, the autocorrelation matrix trace is shown in Figure 5. Different weighting factors, adaptation gains in Eq. (28), error signal, and dynamic learning factor are demonstrated in Figures 6a, 6b, 6c, and 6d respectively.

The reactive power of the system and the load without TSC and with usual TSC along with the proposed TSC are shown in Figures 7a and 7b, respectively. It was assumed that EAF2 is connected to bus 2 at the third second. By considering this condition, the different variations in the power system and TSC in the worst conditions can be analyzed. According to this figure, although the usual TSC has desirably compensated the power system reactive power, the proposed TSC can decrease the reactive power variations, and the system reactive power is around zero.

The voltage and current curves of the 1st, the 8th, and the 16th step of TSC are shown in Figures 8a, 8b, and 8c, respectively. These figures show that the instantaneous amount of voltage and current when cutting and connecting the capacitor steps is about zero, according to the control system design.

The power factor of the power system at bus 1, before and after compensating system, is shown in Figure 9. It is concluded from this figure that, first, the power factor changes are highly reduced by the predicted TSC, and second, the value of this parameter is fixed at about 1, which is highly desirable.

To show the voltage fluctuations of the PCC bus, the IEC flicker meter suggested in [17] is modeled. Therefore, the voltage flicker changes include the instantaneous flicker level (IFL) and the short-term flicker perceptibility (Pst) shown in Figures 10a and 10b without TSC and with the usual and predicted TSC. As can be seen, the proposed compensator can compensate the voltage flicker in bus 1 and, therefore, the voltage fluctuations are improved in this bus.

As was mentioned above, the passive harmonic filters are designed to compensate the current harmonics due to EAFs for the protection of the banks of capacitors. In the KHSC power system, the 2nd, 3rd, 4th,

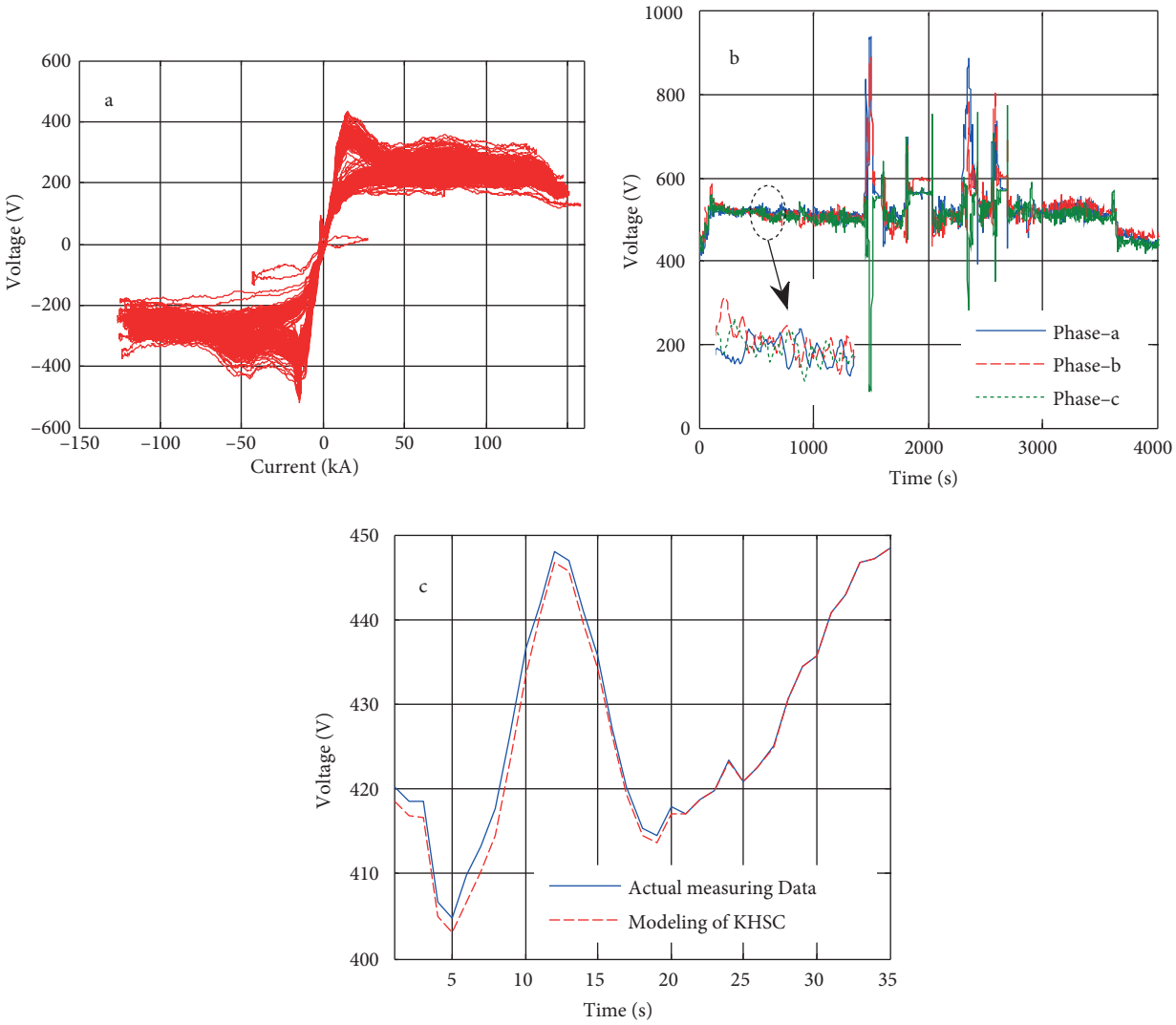


**Figure 4.** Investigating power system modeling of the secondary of one complete melting cycle: a) voltage-current characteristic based on HMM model, b) 3-phase voltage, c) comparison between actual measuring data and modeling of KHSC power system.

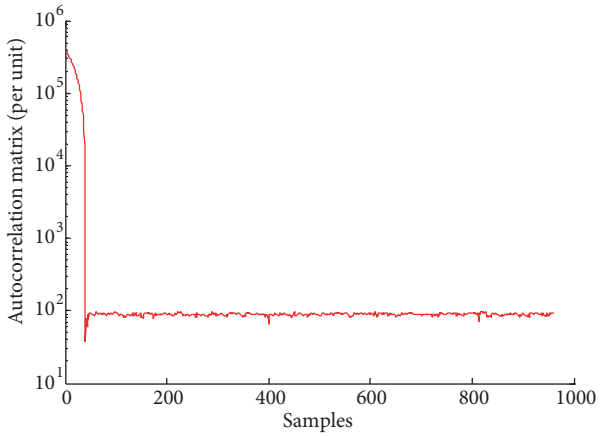


**Figure 5.** Autocorrelation matrix trace.

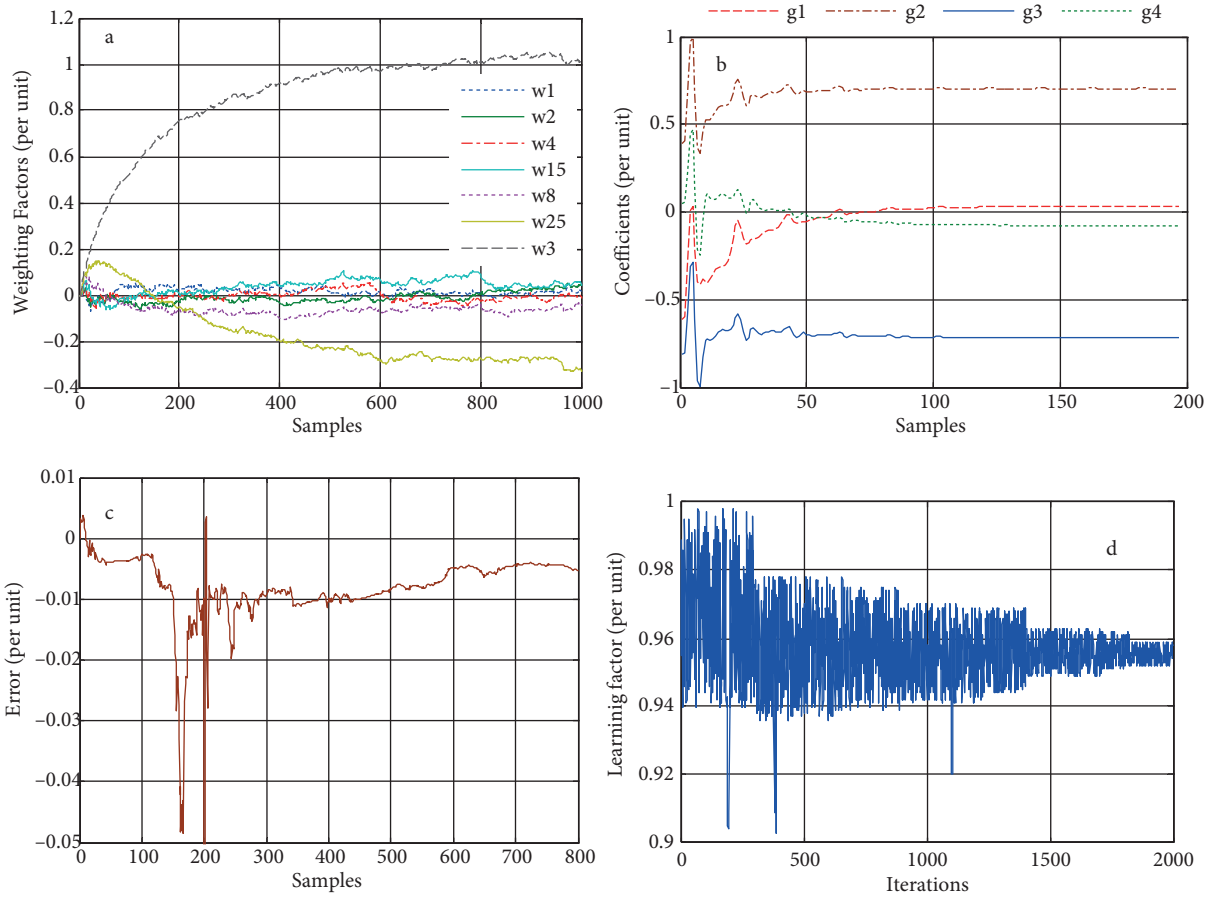


**Figure 6.** Different parameters of proposed delay-less method: a) different weighting factors, b) adaptation gains, c) error signal, d) learning factor changes.

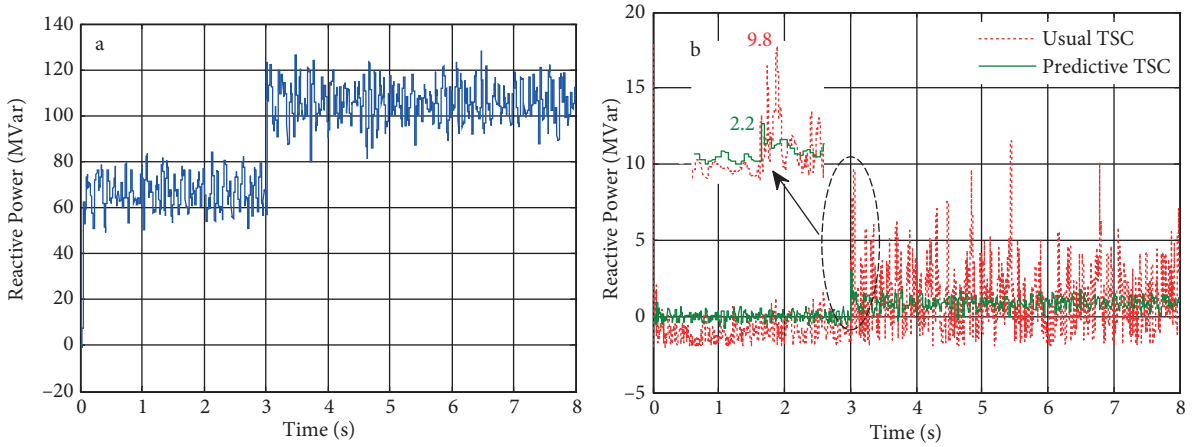


**Figure 7.** Reactive power curve: a) without TSC, b) with usual TSC and predicted TSC.

and 5th order harmonic filters are used for this goal. With regard to the KHSC power system, the frequency characteristics of these filters and system impedance are indicated in Figure 11. It should be noted that this characteristic is very important for the EAF operator to analyze the resonance phenomenon. For example, if

the 4th order harmonics filter is disconnected the operator should remove the 5th order filter; otherwise, it may incur resonance due to high magnitudes of different harmonics of EAF. This figure also shows the intersection of system impendence and designed harmonic filters.

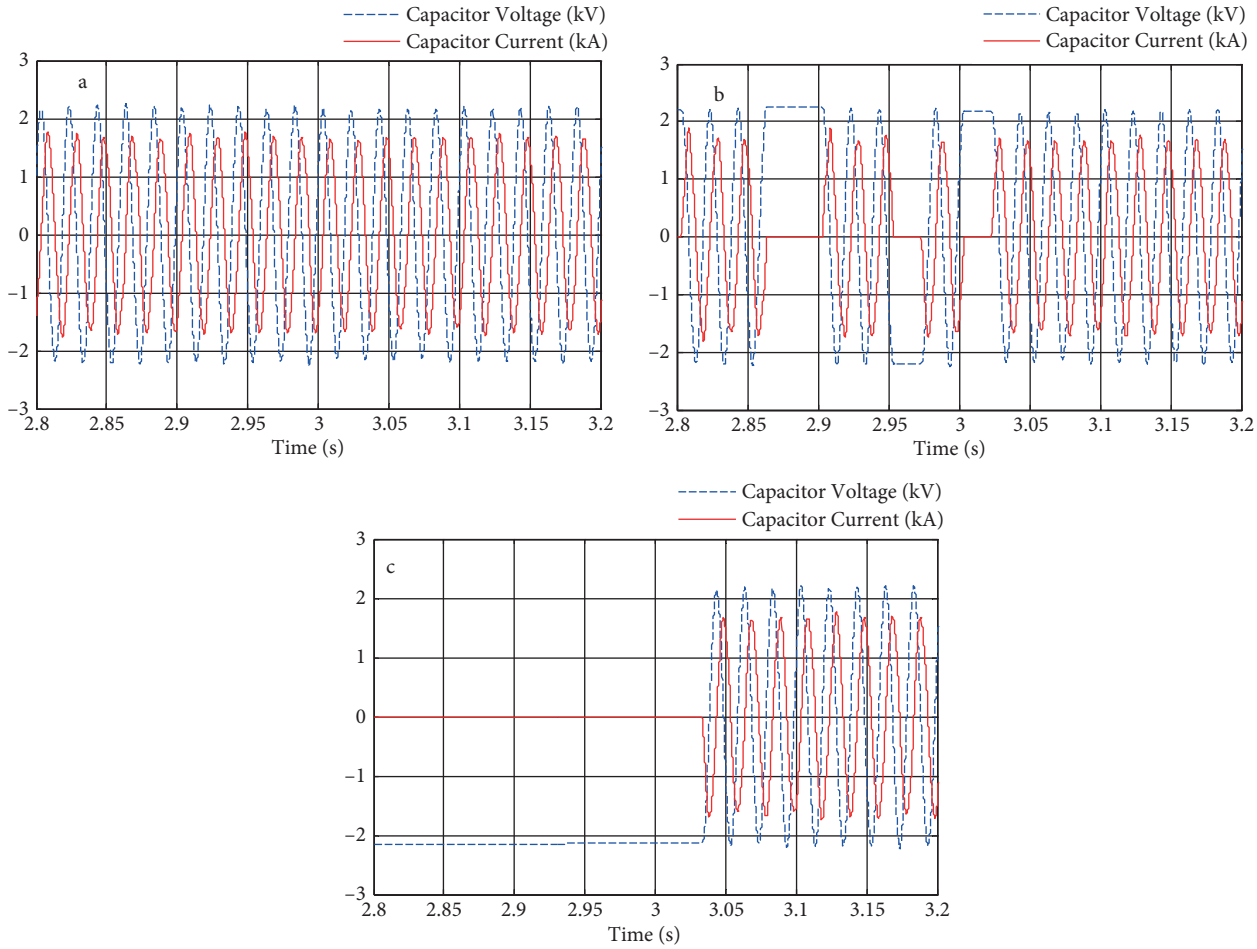


**Figure 8.** Voltage and current curves of: a) first, b) eighth, c) sixteenth steps of capacitors.

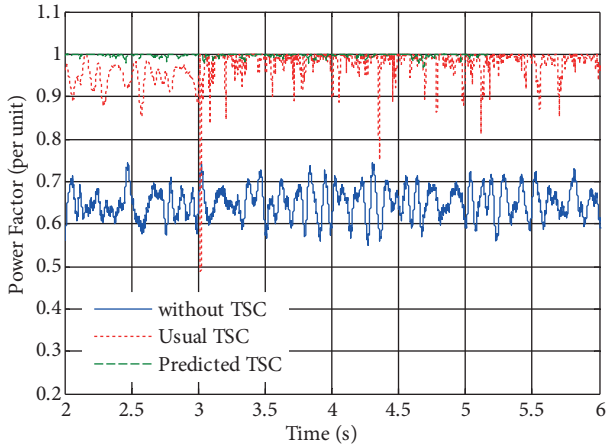


**Figure 9.** Power factor of power system at bus 1 under different conditions.

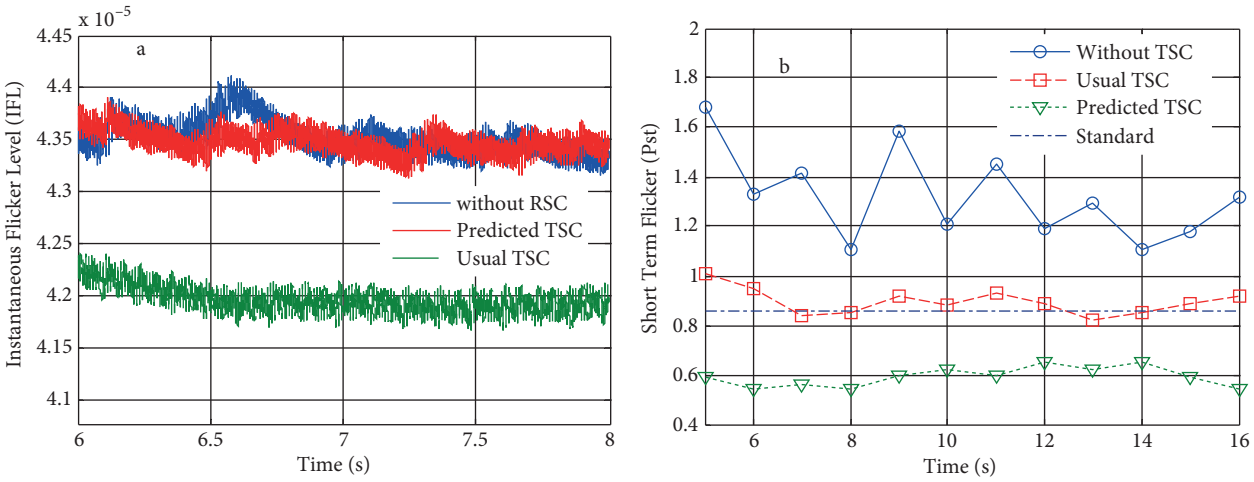


**Figure 10.** Voltage flicker curve: a) IFL, b) Pst in different states.

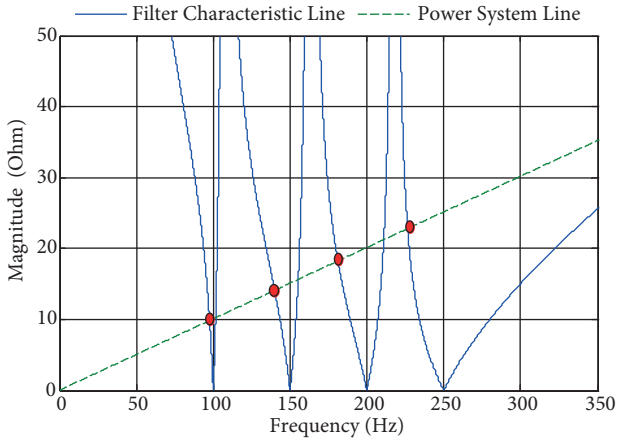


**Figure 11.** Magnitude of power system and filter characteristic line.

Considering the experimental and modeling results in this section, it can be seen that the proposed compensator has desirably compensated the reactive power, power factor, and voltage flicker. They also led to the following:

1) The proposed EAF model based on HMM and data collection can generate the effects of the actual KHSC power system such as voltage flicker, harmonics, etc. Therefore, based on experimental results the presented model can be reliably used for investigating predicted TSC.

2) The experimental results indicate they can be used with the ARMA models and EAF modeling. Table 2 shows the different models of ARMA with various errors compared with standards. Therefore, the selected ARMA, which has been calculated by one cycle window, is based on the actual measurement of the voltage and current of EAFs that can predict the reactive power of EAFs. Then the RLS-DLF can update the different coefficients of the obtained ARMA (2,1). Without the experimental results, calculating the ARMA model for EAF reactive power is impossible or very difficult.

3) The advantages of the proposed method are: 1) An increase in the TSC performance speed compensates the reactive power and voltage flicker. 2) It is not required to replace the existing control strategy;

it is sufficient to only implement the proposed method by means of the DSP modules. 3) In the previous method, Eq. (1) was used to calculate the reactive power fundamental; the proposed method is implemented more easily for each stage. 4) The ARMA coefficients' error is very low using the experimental results in the proposed method.

## 5. Conclusion

In this paper, first a power system with the 2 EAFs was completely designed and simulated as a case study. Then the EAF was modeled based on the HMM method. In the next step, a TSC compensator for this system was designed. To omit the time delay resulting from the TSC's natural performance, the proposed predictive method based on ARMA and RLS-DLF was presented. In this process, a reactive power measurement system with suitable speed and accuracy was proposed. By using this parallel compensator, the reactive power of the overall system was kept constant within a desirable limit, and the voltage flicker was mitigated in an acceptable manner. The experimental results verify the correctness of this approach. Additionally, designing the harmonic filters brought about a reduction of the harmonic components, their distortions, and the resonance effect in the power system. The proposed TSC was implemented in the KHSC.

As previously expressed, the KHSC is a large steel company with 2 EAFs per busbar and 1 TSC. The disadvantage of this compensator is a time delay of about 20 ms in its response time. This delay means that the compensator cannot improve the voltage flicker and reactive power very well. Therefore, by using the proposed method, the TSC performance is significantly enhanced at low cost.

## References

[1] Alonso MAP, Donsion MP. An improved time domain arc furnace model for harmonic analysis. IEEE T Power Deliver 2004; 19: 367-373.

[2] Mousavi Agah SM, Hosseinian SH, Askarian Abyaneh H, Moaddabi N. Parameter identification of arc furnace based on stochastic nature of arc length using two-step optimization technique. IEEE T Power Deliver 2010; 25: 2859-2867.

[3] Gol M, Salor O, AlboyacıB, Mutluer B, ÇadırcıI, Ermi M. A new field-data-based EAF model for power quality studies. IEEE T Ind Appl 2010; 46: 1230-1242.

[4] Beites LF, Mayordomo JG, Hernandez A, Asensi R, Harmonics, inter harmonic, unbalances of arc furnaces: a new frequency domain approach. IEEE T Power Deliver 2001; 16: 661-668.

[5] Torabian Esfahani M, Vahidi B. A new stochastic model of electric arc furnace based on hidden Markov model: a study of its effects on the power system. IEEE T Power Deliver 2012; 27: 1893-1901.

[6] Parniani M, Mokhtari H, Hejri M. Effects of dynamic reactive compensation in arc furnace operation characteristics and its economic benefits. In: Transmission and Distribution Conference and Exhibition Conference; 6–10 October 2002. pp. 1044-1049.

[7] Depormmier B, Stanley J. Static var compensator upgrade in a steel mill. In: Power Engineering Society General Meeting; 13–17 July 2003; Toronto, Canada. pp. 362-365.

[8] Sheng X, Jian-Feng Z, Guo-Qing T. A new SVC control strategy for voltage flicker mitigation and integrated compensation to electric arc furnace. In: Third International Conference on Electric Utility Deregulation and Restructuring and Power Technologies; 6–9 April 2008; Nanjing, China. pp. 1972-1976.

[9] Wang YF, Jiang JG, Ge LS, Yang XJ. Mitigation of electric arc furnace voltage flicker using static synchronous compensator. In: 5th International Power Electronics and Motion Control Conference; 14–16 August 2006; Shanghai, China. pp. 1-5.

[10] Garcia-Cerrada A, Garcia-Gonzalez P, Collantes R, Gomez T, Anzola J. Comparison of thyristor-controlled reactors and voltage-source inverters for compensation of flicker caused by arc furnaces. IEEE T Power Deliver 2000; 15: 1225-1231.

[11] Chow TW. Measurement and evaluation of instantaneous reactive power using neural networks. IEEE T Power Deliver 1994; 9: 1253-1260.

[12] Yoon WK, Devaney MJ. Reactive power measurement using the wavelet transform. IEEE T Instrum Meas 2000; 49: 246-252.

[13] Gomez-Martinez MA, Medina A, Fuerte-Esquivel CR. AC arc furnace stability analysis based on bifurcation theory. IEE Proc-C 2006; 153: 463-468.

[14] Andrade MT. A new current relay for capacitors in medium voltage LC harmonic filters. In: Transmission and Distribution Conference and Exposition; 8–11 November 2004. pp. 686-690.

[15] Mattavelli P. Design aspects of harmonic filters for high-power AC/DC converters. In: Power Engineering Society Summer Meeting; 16–20 July 2000; Seattle, WA, USA. pp. 795-799.

[16] Samet H, Golshan MEH. Employing stochastic models for prediction of arc furnace reactive power to improve compensator performance. IET Gener Transm Dis 2008; 2: 505-515.

[17] Fregosi D, White LW, Green E, Bhattacharya S, Watterson J. Digital flickermeter design and implementation based on IEC Standard. In: Energy Conversion Congress and Exposition; 12–16 September 2010; Atlanta, GA, USA. pp. 4521-4526.

**A. Appendix.** ACF and PACF of ARMA(p,l).

The most important parameters in achieving an adequate ARMA model are the ACF and PACF of the time series. These parameters are calculated as follows:

$$ACF_j = \frac{\sum_{t=1}^{N-j} (q_t - \mu)(q_{t+j} - \mu)}{\sum_{t=1}^{n} (q_t - \mu)^2} \quad j = 1, 2, 3, ... \tag{A.1}$$

$$PACFj = \begin{cases} ACF1j = 1 \\ \frac{ACF1 - \sum^{ACF_{j-1,h} ACF_{j-h}}}{1 - \sum_{h=1}^{j-1} ACF_{j-1,h} ACF_h} \quad j = 2, 3, ... \end{cases} \tag{A.2}$$

where

$$ACF_{j,h} = ACF_{j-1,h} - PACF_j ACF_{j-1,j-h} h = 1, 2, ..., k-1.$$

**B. Appendix.** Weighting factors.

The weighting factors are calculated as:

$$\omega_{k-1} = AF_{k-1}^{-1} CF_{k-1} \tag{B.1}$$

$$\begin{aligned} \omega_k &= AF_k^{-1} CF_k = (\mu^{-1} AF_{k-1}^{-1} - \mu^{-1} \phi_k X_k^T AF_{k-1}^{-1})(\mu CF_{k-1} + X_k d_k) \\ &= \omega_{k-1} + \phi_k (d_k - X_k \omega_{k-1}) = \omega_{k-1} + \phi_k e_k \end{aligned} \tag{B.2}$$

where

$$\begin{aligned} \phi_k &= \mu_{-1} AF_{k-1}^{-1} X_k - \mu_{-1} \phi_k X_k^T AF_{k-1}^{-1} X_k \\ &= (\mu^{-1} AF_{k-1}^{-1} - \mu^{-1} \phi_k X_k^T AF_{k-1}^{-1}) X_k \\ &= AF_k^{-1} X_k \end{aligned}$$